Attachment A –

Sound Exposure Modelling for the Bight 3D seismic survey in the eastern Great Australian Bight, South Australia. Prepared by CMST. Report C2012-36, 23 July 2012

Curtin

UNIVERSITY OF TECHNOLOGY

Centre for Marine Science and Technology

Sound exposure modelling for the Bight 3D seismic survey in the eastern Great Australian Bight, South Australia

By:

Iain Parnum and Alec J Duncan

Prepared for:

John R Hughes Geophysical Pty Ltd

On behalf of Bight Petroleum

PROJECT CMST 1085

REPORT C2012-36

23 July 2012

Abstract

The Bight Marine 3D Seismic Survey is planned for a region in the eastern Great Australian Bight.

CMST has carried out source level and transmission loss modelling from 8 to 1000 Hz in order to predict the receive levels at ranges up to 200 km away from three source locations.

Horizontal plane source strength is estimated for PGS 3090 in^3 and PGS 4130 in^3 arrays using CMST's numerical seismic source model.

The maximum received SEL is predicted to drop below 160 dB re 1 $\mu Pa^2.s$ at ranges varying between 800 m and 7 km depending on the location of the source and the direction of propagation. The maximum received SELs at the 50 m contour just off the coast of Kangaroo Island (KI) are predicted to be less than 120 dB re 1 μPa^2s, with the smaller array producing received levels approximately 5 dB lower than the larger array. Results from modelling indicate that the maximum received SELs just off the coast of the Eyre Peninsula will be less than 120 dB re 1 μPa^2s, with the smaller array again producing received levels approximately 5 dB lower than the larger array.

The calculated received levels are strongly dependent on water depth, seabed slope, and direction relative to the array. In general, the rate of decay inshore is more rapid then along the contour, but this is counteracted to some extent by the effect of the array directivity, which results in higher source levels in the inshore direction.

Received levels calculated using the modelled source locations should be representative of those that would be produced by the same seismic sources at other locations with similar water depths and seabed slopes.

Table of Contents

List of Tables

List of Figures

1 Introduction

A 3D marine seismic survey is planned for the eastern Great Australian Bight (Figure 1) between January and May 2013.

The Client proposes to deploy either of two different seismic source arrays 1) PGS 3090 in^3 and 2) PGS 4130 in^3 at headings of 120 degrees and 300 degrees.

The Client has contracted *the Centre for Marine Science and Technology* (CMST) to quantitatively model the likely underwater sound levels caused by the survey up to 200 km from the source. Because of the large effect that water depth and seabed slope has on underwater acoustic propagation this was done by computing the geographical distribution of *Sound Exposure Levels* (SEL) due to a single-shot from a seismic source at three representative source locations in the survey area (Figure 1). When plotted relative to the source location, the received levels due to a source at each of these locations are likely to be representative of levels due to a source at similar water depths at other locations in the survey area.

The three source locations in the survey area (P1 to P3) are shown in Figure 1. All three points have been modelled for the PGS 3090 in^3 array and P1 has also been modelled for the PGS 4130 in^3 array as requested by the client. The array was modelled with a heading of 120 degrees.

The areas of particular interest, as indicated by the Client, were the waters close to Kangaroo Island (KI), the location of which is identified in Figure 1. P1 is the closest point in the survey to KI. P2 and P3 are in the middle of the survey area on the 200 m and 2000 m contours, respectively.

Table 1: Source locations P1-P3 modelled.

Point	Latitude (deg. S)	Longitude (deg. E)
P1	35.5964	135.4324
P2	35.5009	134.9263
P3	35.6532	134.7769

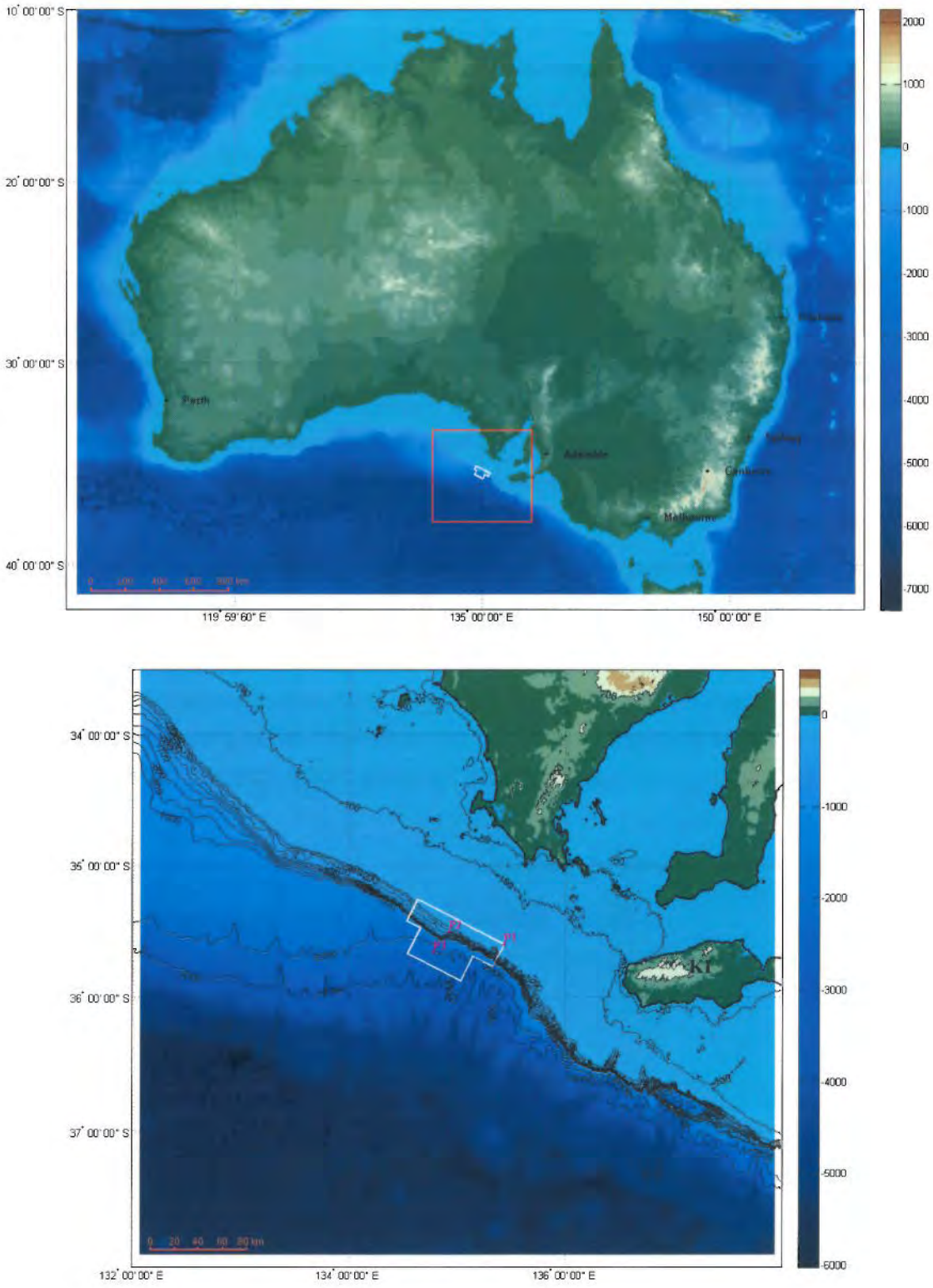

Figure 1: Geographical location of the survey covered by this report. The red box in the top panel shows the location of the bottom panel. The solid white line is the location of the Bight 3D survey. The three source locations (P1-P3) used in the modelling are shown in magenta. The location of Kangaroo Island (KI) is identified in the bottom plot.

2 Methods

2.1 Source modelling

2.1.1 Specification

The Client has specified and provided configuration data for the PGS 3090 in^3 and PGS 4130 in^3 airgun source array. The array depth is 6 m for both systems.

2.1.2 Modelling and calibration methods

Acoustic signals required for this work were synthesised using CMST's numerical model for airgun arrays. The procedure implemented for each individual source element is based on the bubble oscillation model described in Johnson (1994) with the following exceptions:

- An additional damping factor has been added to obtain a rate of decay for the bubble oscillation consistent with measured data;
- The zero rise time for the initial pressure pulse predicted by the Johnson model has been replaced by a finite rise time chosen to give the best match between the high frequency roll-off of modelled and measured signal spectra;
- For the coupled-element model used in this work, the ambient pressure has been modified to include the acoustic pressure from the other guns in the array and from the surface ghosts of all the guns. Including this coupling gives a better match between the modelled signal and example waveforms provided by seismic contractors, but only has a minor influence on the spectrum of this signal and hence on the modelled received levels.

The model is subjected to two types of calibration:

- The first is historical and was part of the development of the model. It involved the tuning of basic adjustable model parameters (damping factor and rise time) to obtain the best match between modelled and experimentally measured signals, the latter obtained during sea trials with CMST's 20 in^3 air gun. These parameters have also been checked against several waveforms from larger guns obtained from the literature.
- The second form of calibration is carried out each time a new array-geometry is modelled, the results of which are presented in section 2.1.3 below. Here, the modelled gun signals' amplitudes are scaled to match the signal energy for a far-field waveform for the entire array computed for the nadir direction (including ghost) to that of a sample waveform provided by the Client's seismic contractor. When performing this comparison the modelled waveform is subjected to filtering similar to that used by the seismic contractor in generating their sample, or additional filtering is applied to both data sets to emphasise a section of the bandwidth of the supplied data which CMST regards as being most reliable.

Horizontal beam patterns for the calibrated array were built up one azimuth at a time as follows:

- The distances from each gun to a point in the far-field along the required azimuth were calculated. (The far-field is the region sufficiently far from the array that the array can be considered a point source);

- The corresponding time delays were calculated by dividing by the sound speed;
- Computed signals for each gun were delayed by the appropriate time, and then these delayed signals were summed over the guns;
- The energy spectral density of the resulting time domain waveform was then calculated via a Fourier transform;
- During this procedure care was taken to ensure that the resulting spectrum was scaled correctly so that the results were in source energy spectral density units: dB re 1 $\mu Pa^2s/Hz$ @ 1m.

2.1.3 Source modelling results

Final model calibration, as described in the section above, was carried out using Client-supplied model waveform for the array at nadir, which has been subjected to a proprietary low-pass filter with f_{3dB} = 300Hz. CMST's model achieved similar filter performance by applying a 1storder low-pass Butterworth filter with f_{3dB} = 300Hz. This resulted in linear calibration factors of 0.805 for PGS 3090 in^3 and 0.64 for PGS 4130 in^3 (based on the square root of integrated spectral energy). The results of CMST's model agree well with the Client-supplied waveforms (Figure 2 and Figure 3).

The azimuth dependent spectra are plotted as beam patterns in Figure 4 and Figure 5. The horizontal-plane frequency-dependent beam-patterns display strong azimuthal dependence at high frequencies and the directionality reflects the two primary axes of symmetry in the array geometry.

An equivalent source level was calculated by integrating the horizontal plane source spectrum over frequency and averaging over azimuth. The value obtained for PGS 3090 in^3 and PGS 4130 in^3 are 228 and 229 dB re 1 μPa^2s @ 1m, respectively. . These values are indicative only, as they obscure important effects such as the frequency dependent directivity of the arrays and interaction of the sound with the sea surface. These equivalent source levels were not used in the calculation of received levels.

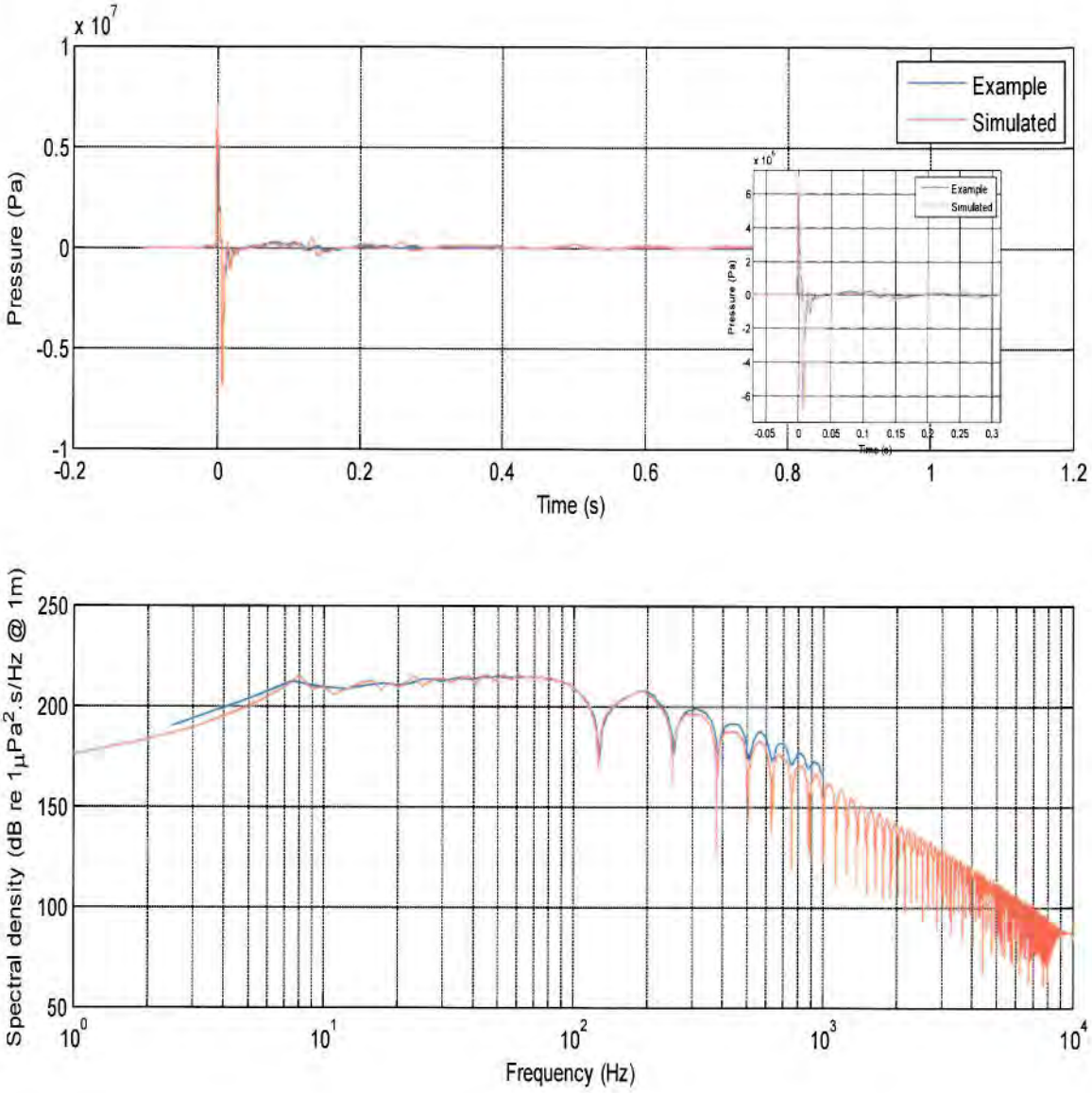

Figure 2: Far field array signals at nadir (inc-ghost) post-calibration using coupled-element for the PGS 3090 in^3 array.

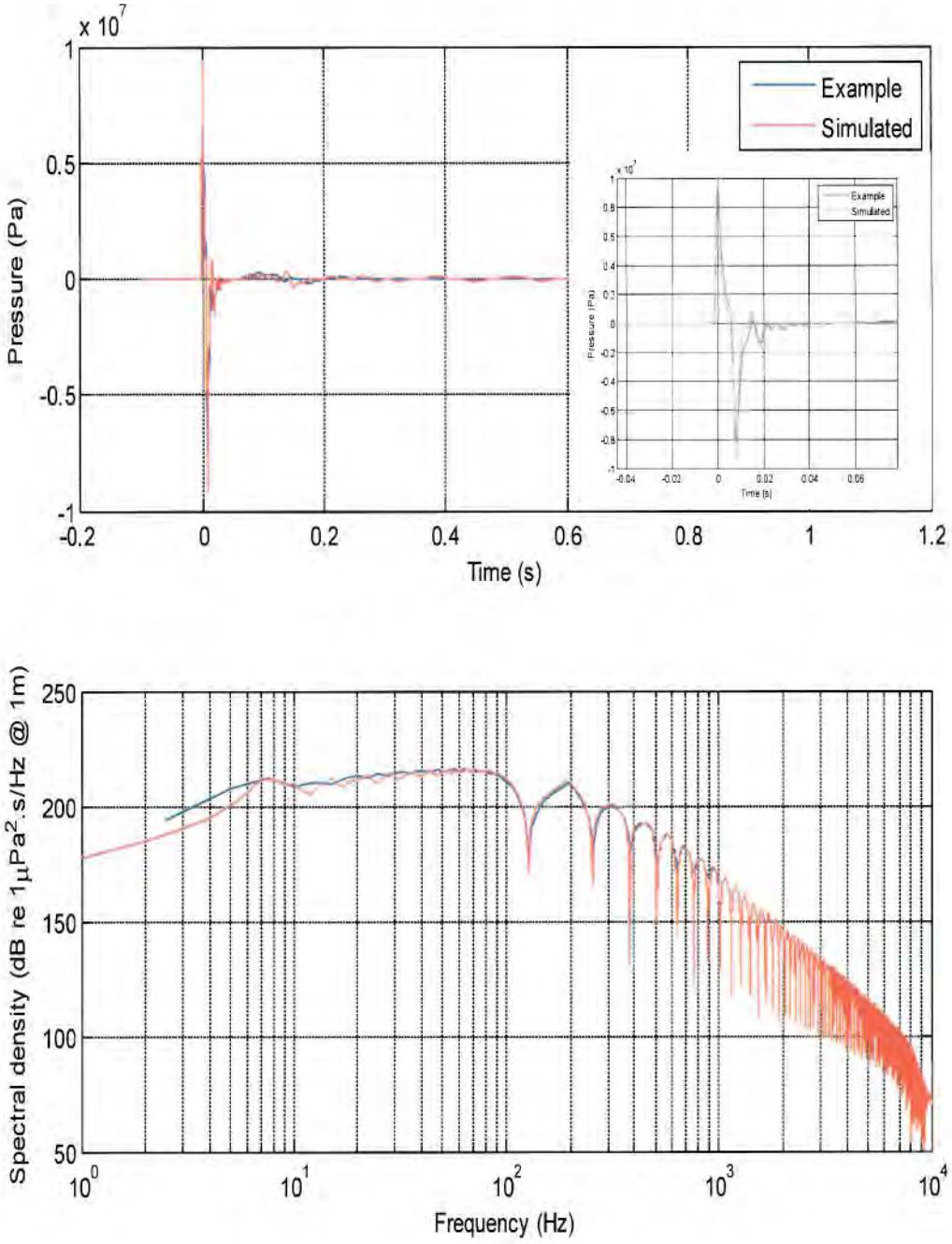

Figure 3: Far field array signals at nadir (inc-ghost) post-calibration using coupled-element for the PGS 4130 in^3 array.

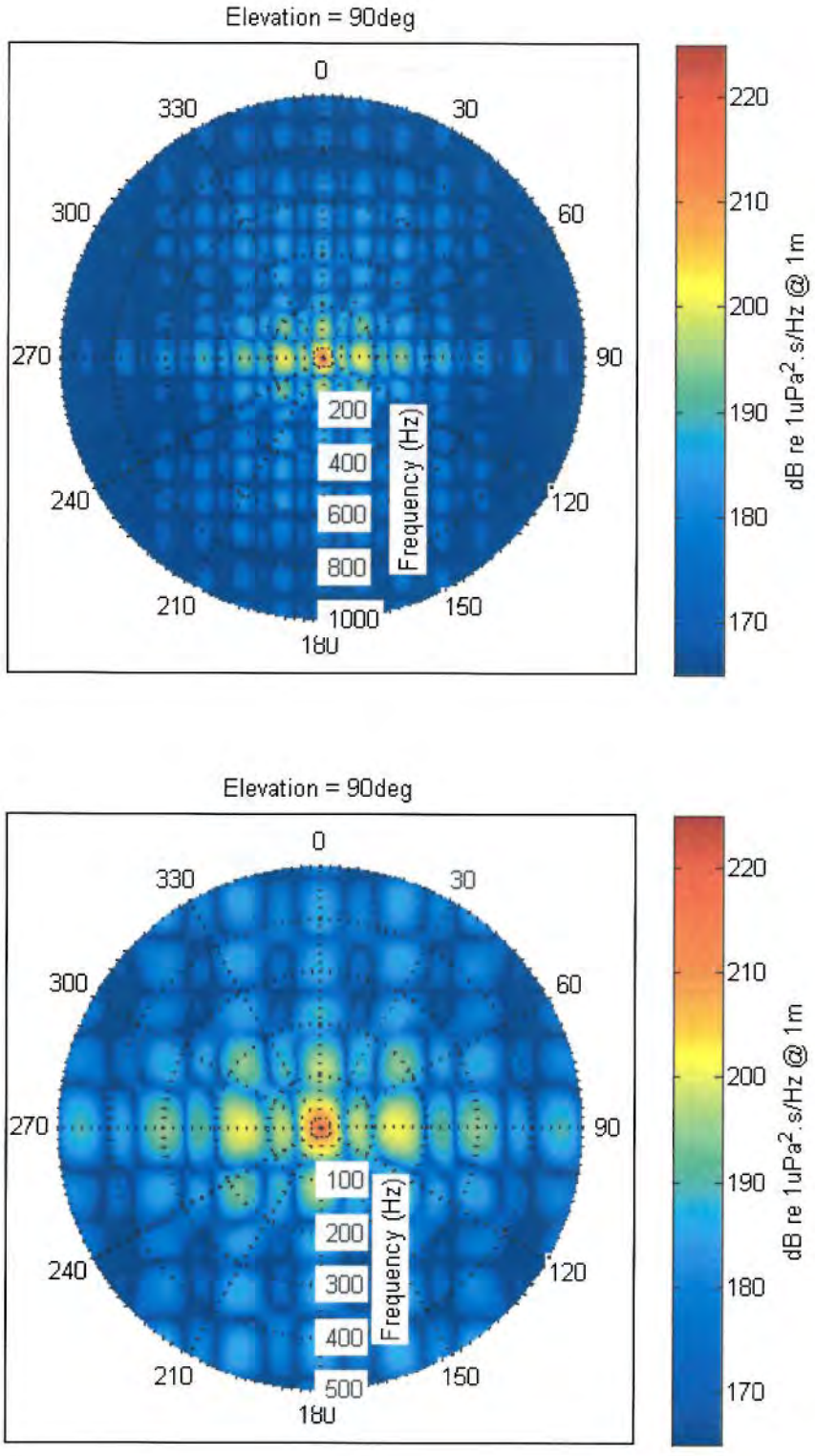

Figure 4: Horizontal plane azimuth-dependent spectral level for model source, ex-ghost. PGS 4130 in^3 array, ϕ=90°, for 0-1000 Hz (top panel) and 0-500 Hz (bottom panel).

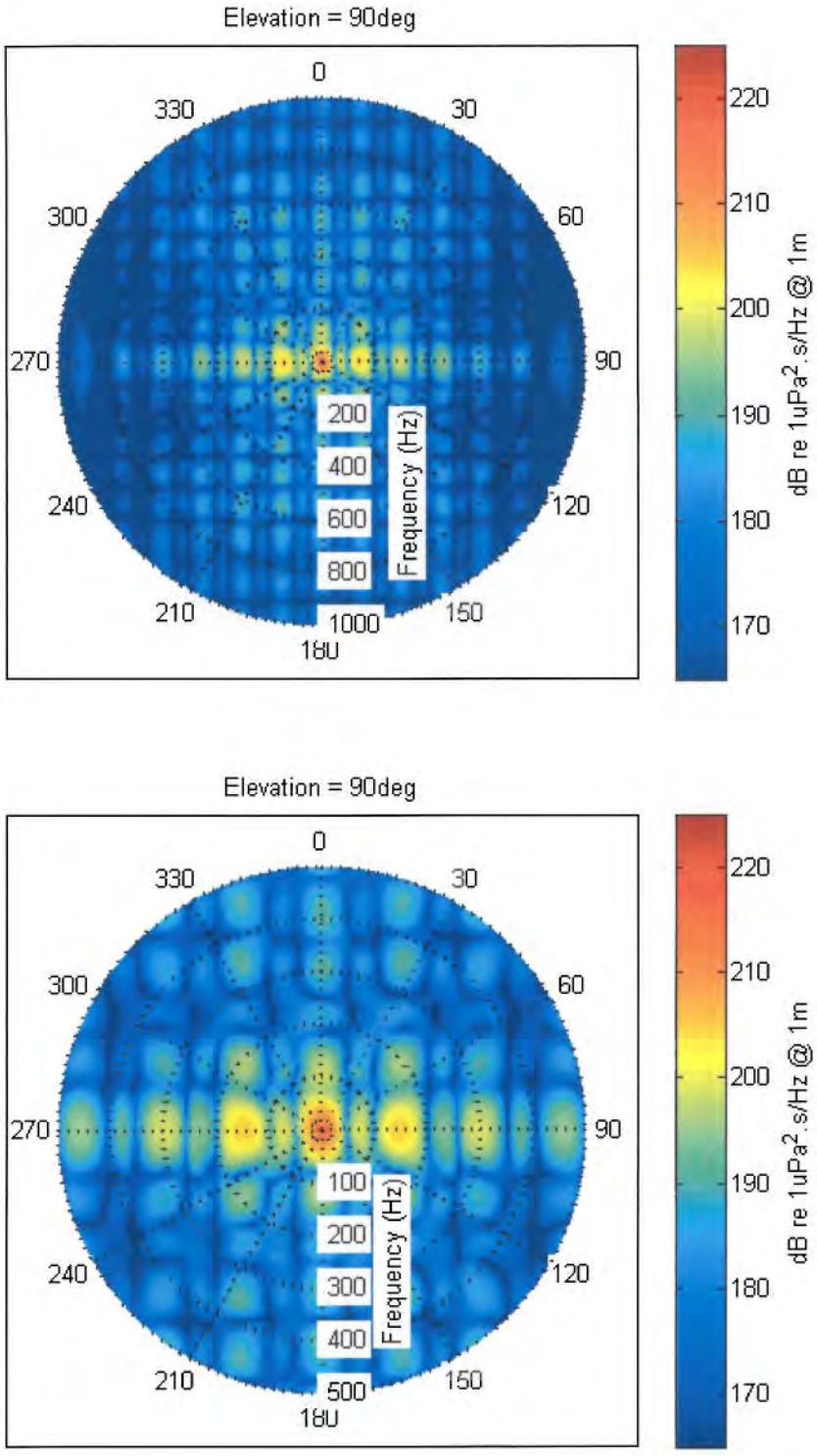

Figure 5: Horizontal plane azimuth-dependent spectral level for model source, ex-ghost. PGS 4130 in^3 array, ϕ=90°, for 0-1000 Hz (top panel) and 0-500 Hz (bottom panel).

2.2 Propagation modelling

2.2.1 Source location & bathymetry

The three source locations selected for this work, P1-P3, were selected to be representative of the different propagation conditions found in the survey area (see Introduction, Table 1). For each point, propagation tracks were defined over absolute azimuths of 0-360°, every 2.5 degrees between 0 and 140° and between 300 and 360°, and every 10° between 140 and 300° (Figure 5). The finer azimuthal sampling was applied inshore, particularly in order to reveal acoustic paths through regions of shallow bathymetric features.

Bathymetry data used in the range-dependent propagation modelling is extracted from the Geoscience Australia Bathymetry (0.15') database along the transects shown in Figure 5. Water level across the entire modelling area has been adjusted uniformly to accommodate the highest quoted value of mean spring tide above mean sea level in the area. That value is +0.75 m at Port Lincoln.

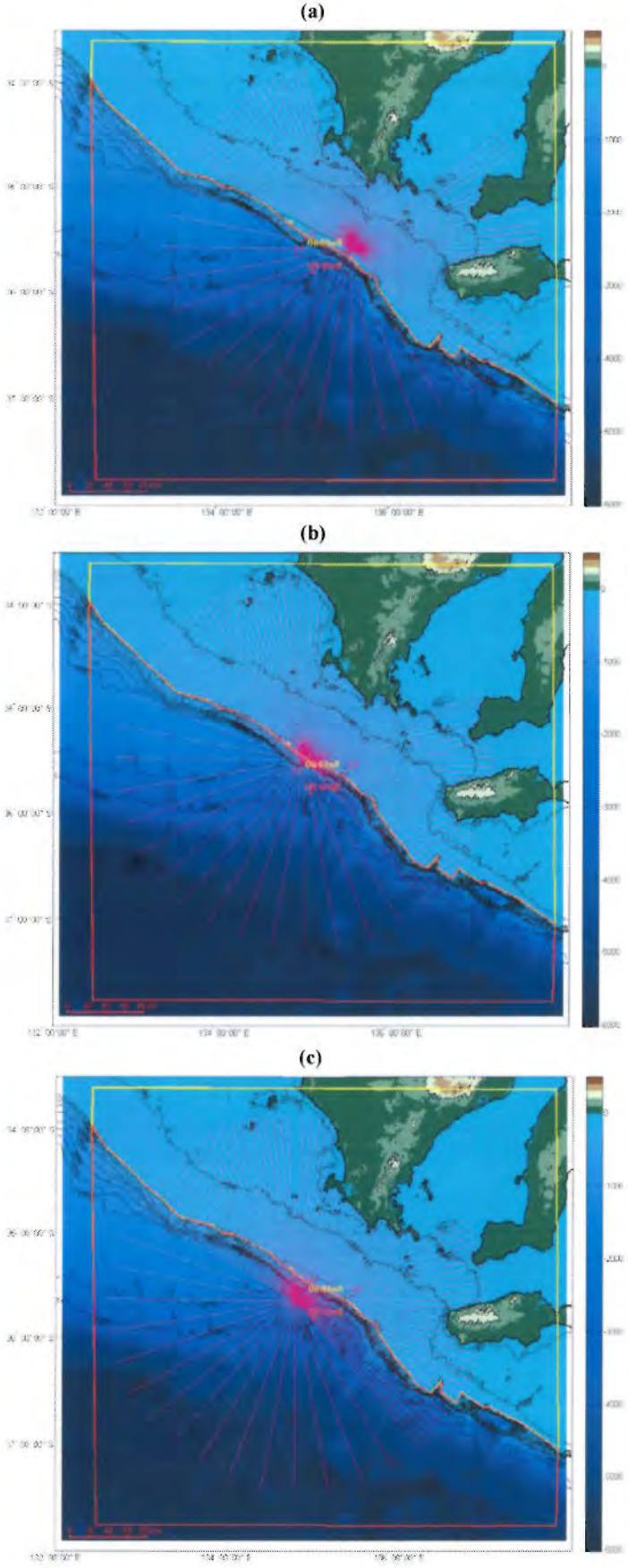

Figure 6: Bathymetry data transects for propagation modelling for source locations at the: (a) closest point to Kangaroo Island (P1), centre of the survey area at: (b) 200 m contour (P2), and (c) 2000 m contour (P3).

The acoustic environment spanned by the propagation model has been spatially partitioned into two sub-domains, primarily to distinguish between acoustically distinct regions:

- on-shelf, and
- off-shelf

The 200m depth contour has been chosen as a convenient boundary for the two model environments (Figure 6). The properties used to describe the water column and seabed environment for each of these regions is given below.

Water-column

The water column properties of each sub-domain are extracted from data for a single reference point in each region. A point is nominated from a region of sufficient depth so that profiles for the required physical-acoustic parameters are adequately defined over the entire sub-domain. These points are then used to (automatically) locate the nearest suitable grid points of the World Ocean Atlas (NOAA, 2005) from which the parameter profiles are extracted. The sound speed profiles used for this work are plotted in Figure 7.

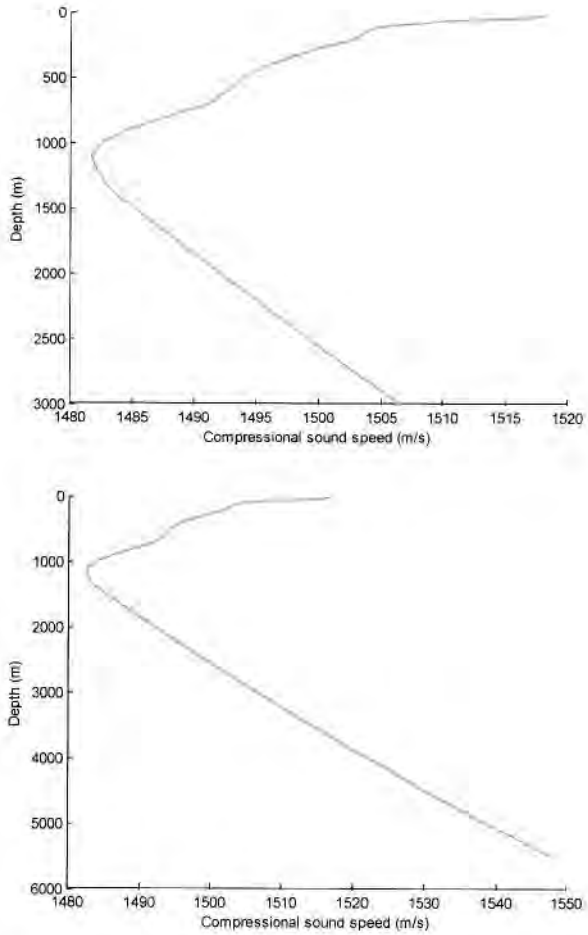

Figure 7: Water column sound speed profiles used by the propagation models: on-shelf (top panel) and off-shelf (bottom panel).

Seabed

The seabed models used here have been proposed by CMST, based on its previous experience with similar environments and the study by James *et al.* (2001). Although the Client was unable to provide a description of the shallow geology of this specific area, these seabed models are consistent with information available for other areas of the Great Australian Bight.

The acoustic seabed models have been selected to avoid direct modelling of an elastic seabed. This is due to the lack of availability of range-dependent propagation codes which are stable for elastic substrates overlain by low shear-wave velocity sediments. Jensen *et al.* (2001) was used as a guide in determining the geoacoustic properties of the seabed model.

The two seabed environments are discussed below and summarised in Table 2.

Table 2: Spatially dependent seabed models.

Region	Depth range (m)	Description
On-shelf	0-200	1 m coarse sand on calcarenite (as equivalent fluid)
Off-shelf	> 200	Silty-sand (shear velocity set to zero)

On-shelf region

The nominal seabed model for the shelf environment is a calcarenite substrate overlain with a layer of unconsolidated material. To represent a worst case, a relatively strongly reflecting seabed was chosen comprising a 1 m thick layer of coarse sand over a calcarenite halfspace. To circumvent the problems associated with using range-dependent elastic seabeds in acoustic propagation models, the calcarenite substrate was modelled using an equivalent fluid model that provided a good reflection coefficient match over a grazing angle range of 0 to 30°. The resulting geoacoustic properties are listed in Table 3.

Off-shelf region

The nominal deep water seabed features a deep upper layer of fine sand or coarse silt. The shear velocity of unconsolidated sediments increases with depth but is sufficiently low in the upper regions for elastic effects to be ignored. The nominated model seabed is therefore a "fine-sand" half-space (see Table 3).

Table 3: Seabed acoustic data used in propagation modelling.

Material	Density ($kg.m^{-3}$)	Compressional wave speed (m/s)	Compressional wave attenuation (dB per wavelength)	Shear wave speed (m/s)	Shear wave attenuation (dB per wavelength)
Limestone	2400	3000	0.1	1500	0.2
Equivalent fluid	2400	1350	14	-	-
Sand	2000	1780	0.7	-	-
Silty-sand	1800	1620	0.9		

2.3 Sound exposure level (SEL) calculations

Sound exposure levels (SEL) were calculated as a function of range, depth and azimuth from each source location as follows:

- Transmission loss was, as detailed in the preceding section, modelled along each track using RAMGeo (fluid Parabolic Equation model) for a set of discrete (bin-centre) frequencies at one-third octave intervals from 8 Hz to 1000 Hz. The bathymetry along the track was extracted from the Geosciences Australia 0.15′ database, and the local acoustic environment was based on the regional partitioning described in the previous section.
- Frequency-dependent source level was obtained by integrating the source spectrum for the appropriate (relative) azimuth over each frequency band. (Band edges were chosen as the geometric means of adjacent frequencies.)
- Source level and transmission loss were then combined to compute the received level as a function of range, depth and frequency. This calculation was carried out on the same azimuthal range as the propagation modelling in 2.5° increments. Corresponding transmission loss data were extracted from the closest available transect (in azimuth) used in the propagation modelling.
- Integrated squared acoustic pressure was calculated for each $1/3^{rd}$-octave spectral bin. These values were summed and converted to decibels to yield SEL.

The acoustic field data is presented in three modes.

- The bulk of the data is visualised by reducing the 3-dimensional sound exposure level to a 2-dimensional field in the horizontal plane with each point representing the maximum SEL across all modelled depths in the water column (SEL_{max}). This is generally sufficient for relatively shallow and either constant or shoaling bathymetry because there is little vertical variation in SEL.
- For propagation tracks of particular interest, vertical slices of the 3-dimensional SEL field are plotted along those azimuths. Scale and resolution are the same as for the horizontal plane plots.

3 Results

Geographical distributions of the maximum SEL up to a radius of 200km for the closest point to KI (P1) for the PGS 3090 in^3 and 4130 in^3 arrays are plotted in Figure 8; and, for the points in the centre of the survey area at the 200 m contour (P2) and the 2000 m contour (P3) for the PGS 3090 in^3 array in Figure 9. These plots clearly demonstrate the rapid decay in levels with range that occurs in shallow water compared to deep water. This is particularly pronounced in this instance because the seabed in this area is quite rough, which further increases the decay rate. The plots also show a strong seabed slope dependence, with levels decaying much more rapidly upslope than downslope. The directionality of the airgun array itself is also apparent in Figure 8 and Figure 9, which produces higher levels in the cross-line (i.e. broadside) and along-line (i.e. straight ahead) directions than at intermediate angles.

The maximum SEL versus range for all azimuths for the closest point to KI (P1) for both arrays is shown in Figure 10 and for selected azimuths in Figure 11; and for the points in the centre in the centre of the survey area at the 200 m contour (P2) and the 2000 m contour (P3) using the PGS 3090 in^3 array in Figure 12. In each of the plots the results are compared with a spherical spreading curve based on a nominal source level of 228 and 229 dB re 1 $\mu Pa^2.s$ @ 1m for the PGS 3090 in^3 and PGS 4130 in^3, respectively. These plots show that levels at ranges less than 1km are higher in shallow water than in deep water, but that this trend reverses for ranges more than a few tens of kilometres.

The SEL in the vertical plane from P1 at azimuths of 120° (i.e. straight ahead), 30° (i.e. broadside upslope), 210° (i.e. broadside downslope) and 105° (i.e. towards KI) using the PGS 3090 in^3 and PGS 4130 in^3 arrays are shown in Figure 13 to Figure 16. The maximum SEL in both the vertical and horizontal planes for both the PGS 3090 in^3 and PGS 4130 in^3 arrays from P1 are very similar, which is to be expected since the source levels are within 1 dB of each other. From P1 on an azimuth of 105° (i.e. towards KI) the maximum SEL drops to less than 120 dB re 1 $\mu Pa^2.s$ at a range of 100 km from the source for both arrays.

The SEL in the vertical plane from P2 and P3 at azimuths of 120° (i.e. straight ahead), 30° (i.e. broadside upslope), and 210° (i.e. broadside downslope) using the PGS 3090 in^3 array are shown in Figure 17 to Figure 19. The very different decay rates that occur in the up-slope and down-slope directions are very apparent in Figure 8 to Figure 19. Upslope the rays steepen on each successive reflection from the seabed, resulting in more and more frequent interactions that attenuate the signal; whereas, downslope the energy is being coupled into the deep sound channel after which it has little interaction with the sea surface or seabed, and so decays at a very slow rate.

Deep sound channel propagation is occurring in all directions from P3 (Figure 19 – bottom panel), which is at the offshore end of the survey area. However, because the source is near the surface, and the warm surface waters result in a relatively high sound speed, the sound cycles over almost the entire water column, resulting in slightly lower levels than down-slope from P2 (Figure 19 – top panel).

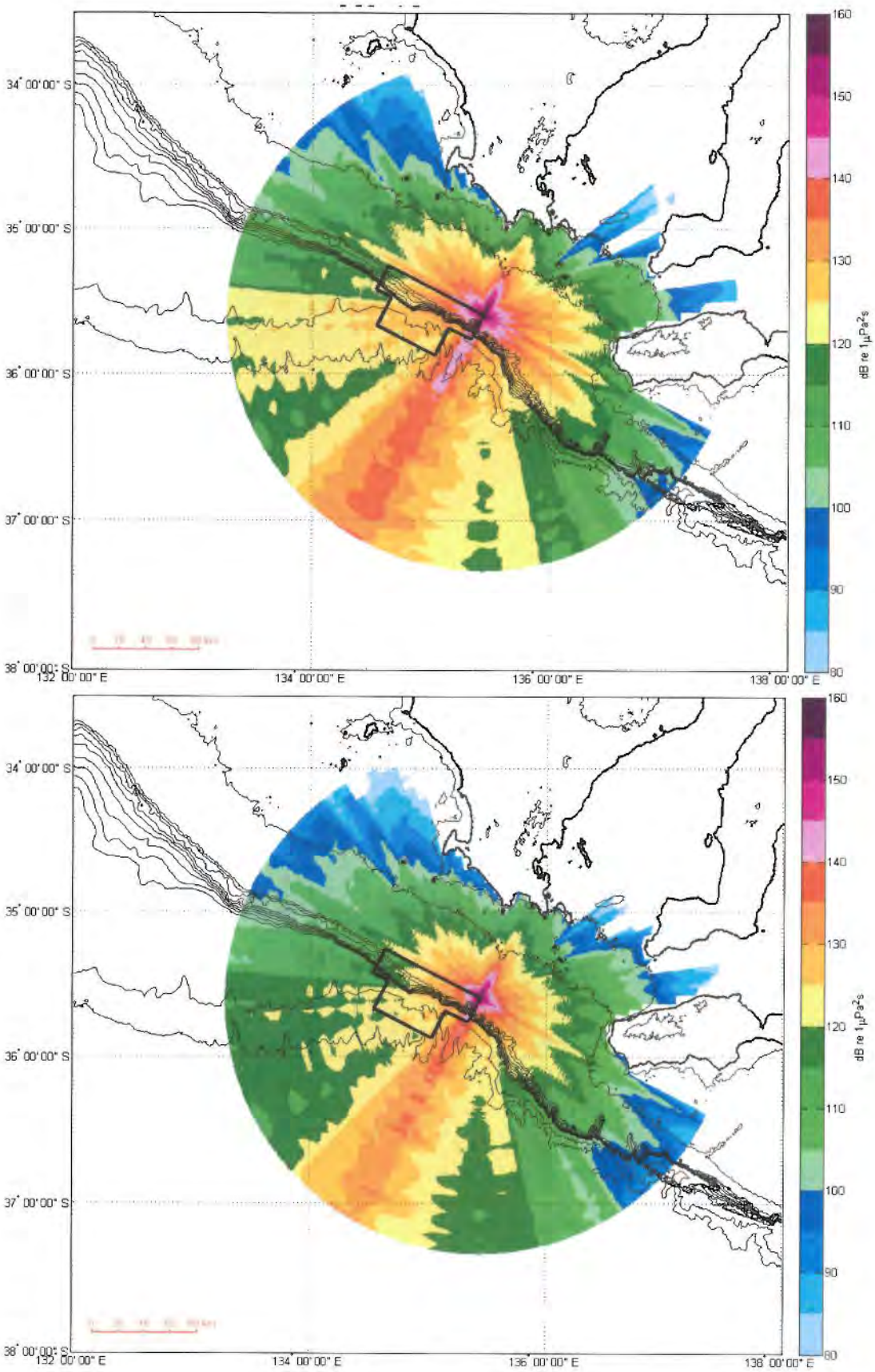

Figure 8: Maximum received sound exposure level at any depth, SELmax(r, θ), for the source location closest to Kangaroo Island (P1) with the: PGS 4130 in^3 array (top panel) and PGS 3090 in^3 array (bottom panel).

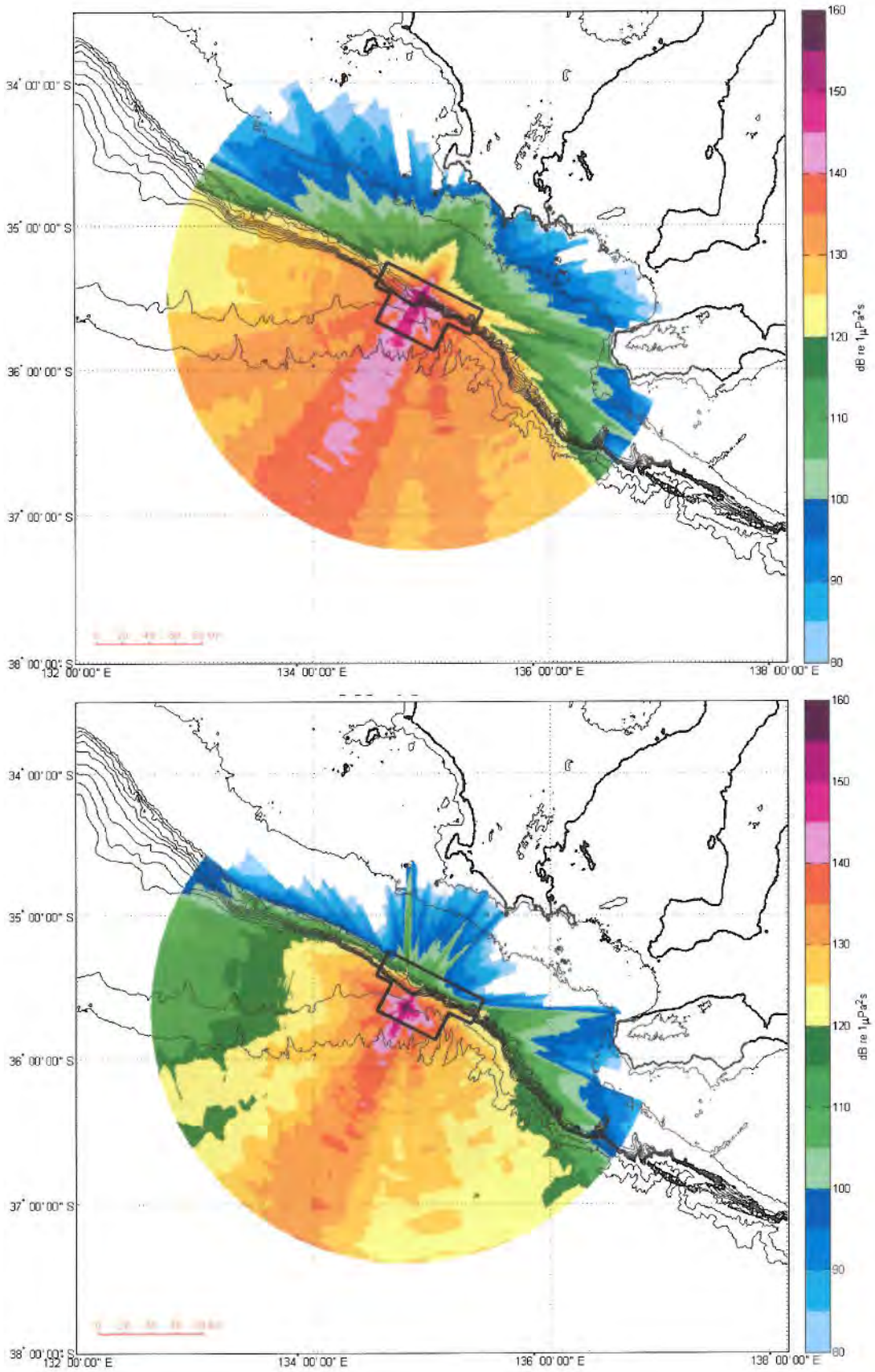

Figure 9: Maximum received sound exposure level at any depth, SELmax(r, θ) for the PGS 3090 in^3 array located in the centre of the survey area at: (P2) the 200 m contour (top panel), and (P3) the 2000 m contour.

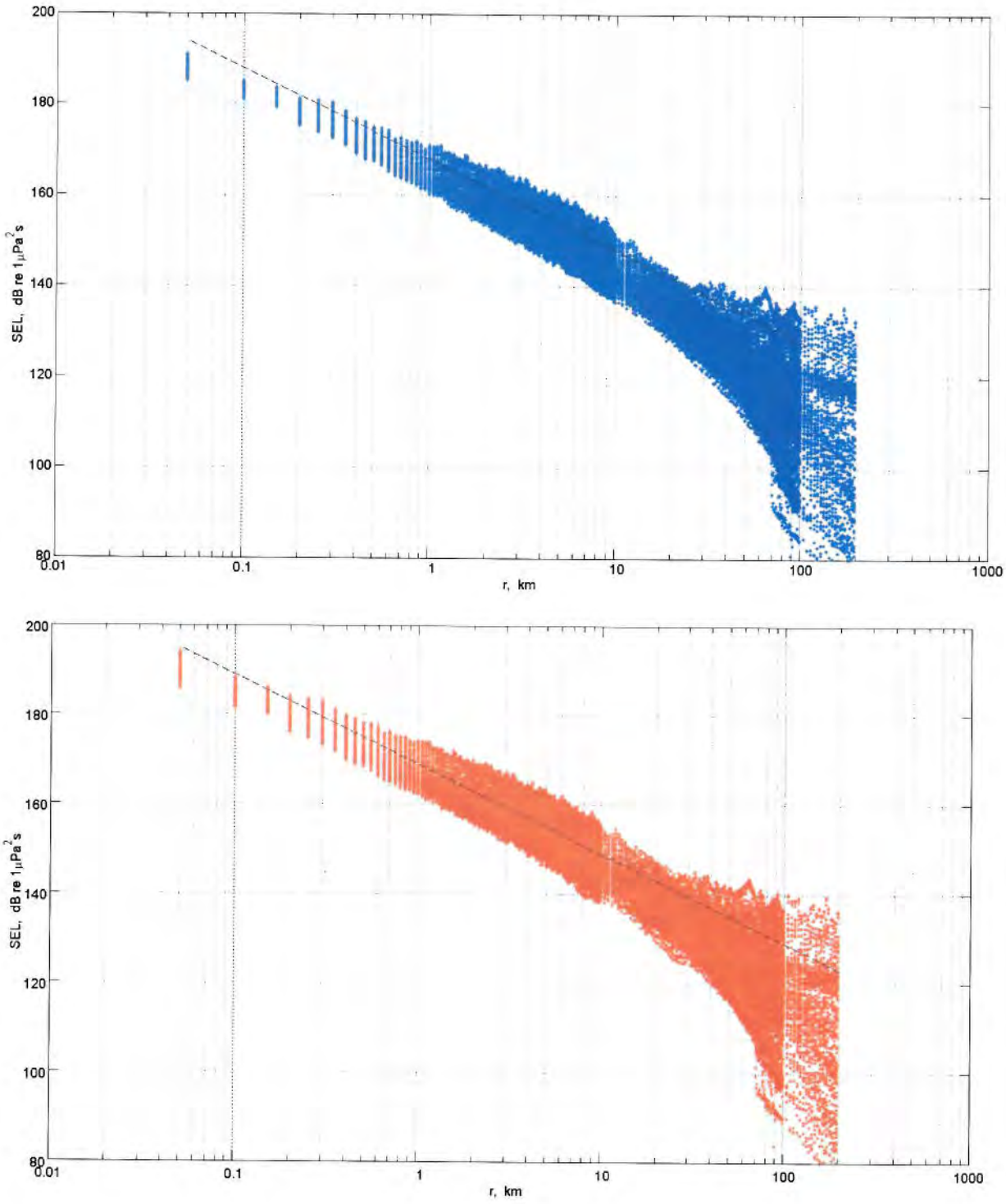

Figure 10: Maximum received sound exposure level at any depth, SEL_{max}, versus range for the closest point to Kangaroo Island (P1): with (top panel) PGS 3090 in^3 array (blue dots) and black dashed line is 228 – spherical spreading loss; and PGS 4130 in^3 array (red dots) and black dashed line is 229 – spherical spreading loss; and (bottom panel).

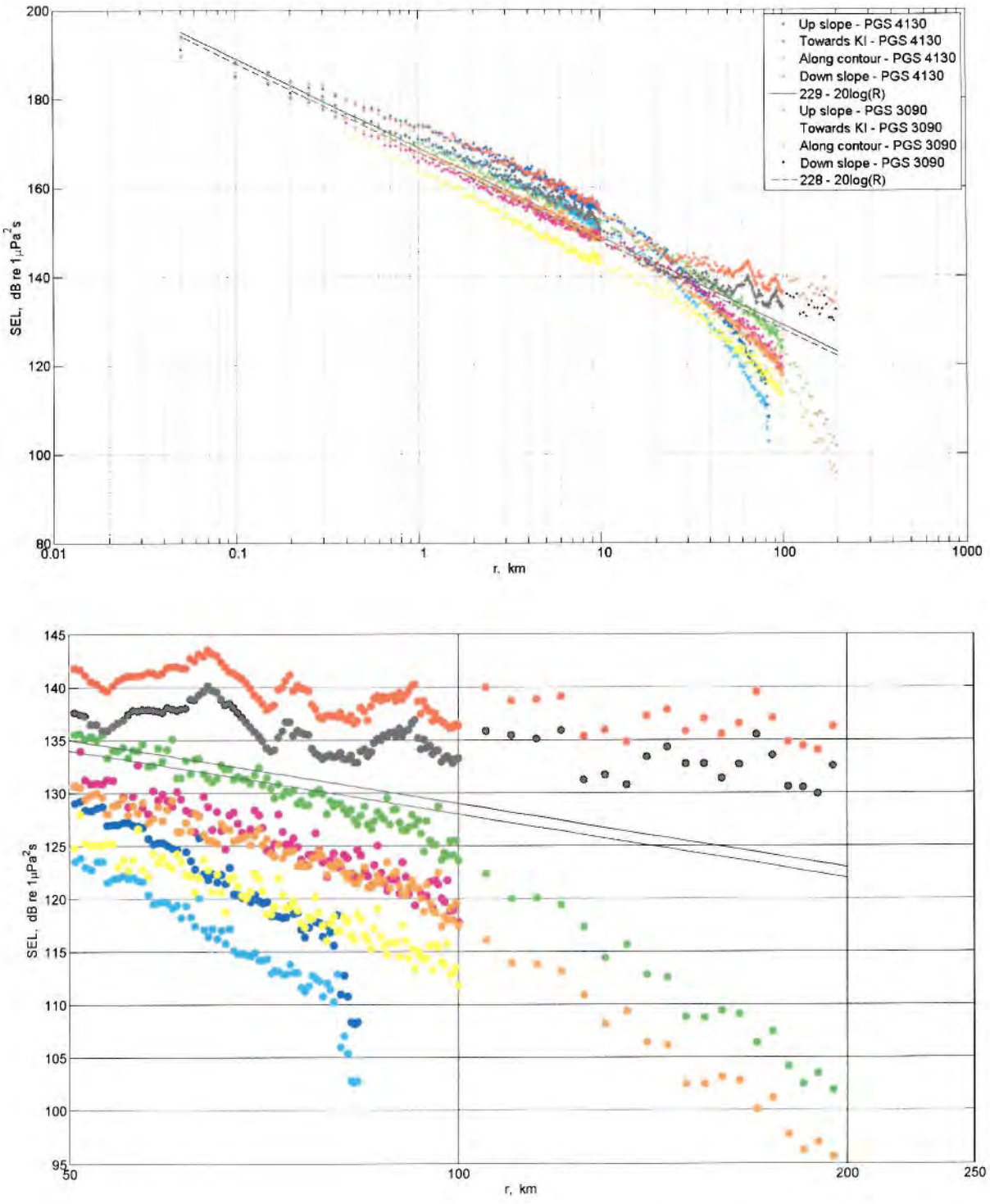

Figure 11: Maximum received sound exposure level at any depth, SEL_{max}, versus range for the closest point to Kangaroo Island (P1) PGS 4130 in^3 and PGS 3090 in^3 arrays for the directions upslope (30°), downslope (210°) and along contour (120°). Black solid line is 229 – spherical spreading loss; and black dashed line is 228 – spherical spreading loss. The bottom panel shows the end part of the lines.

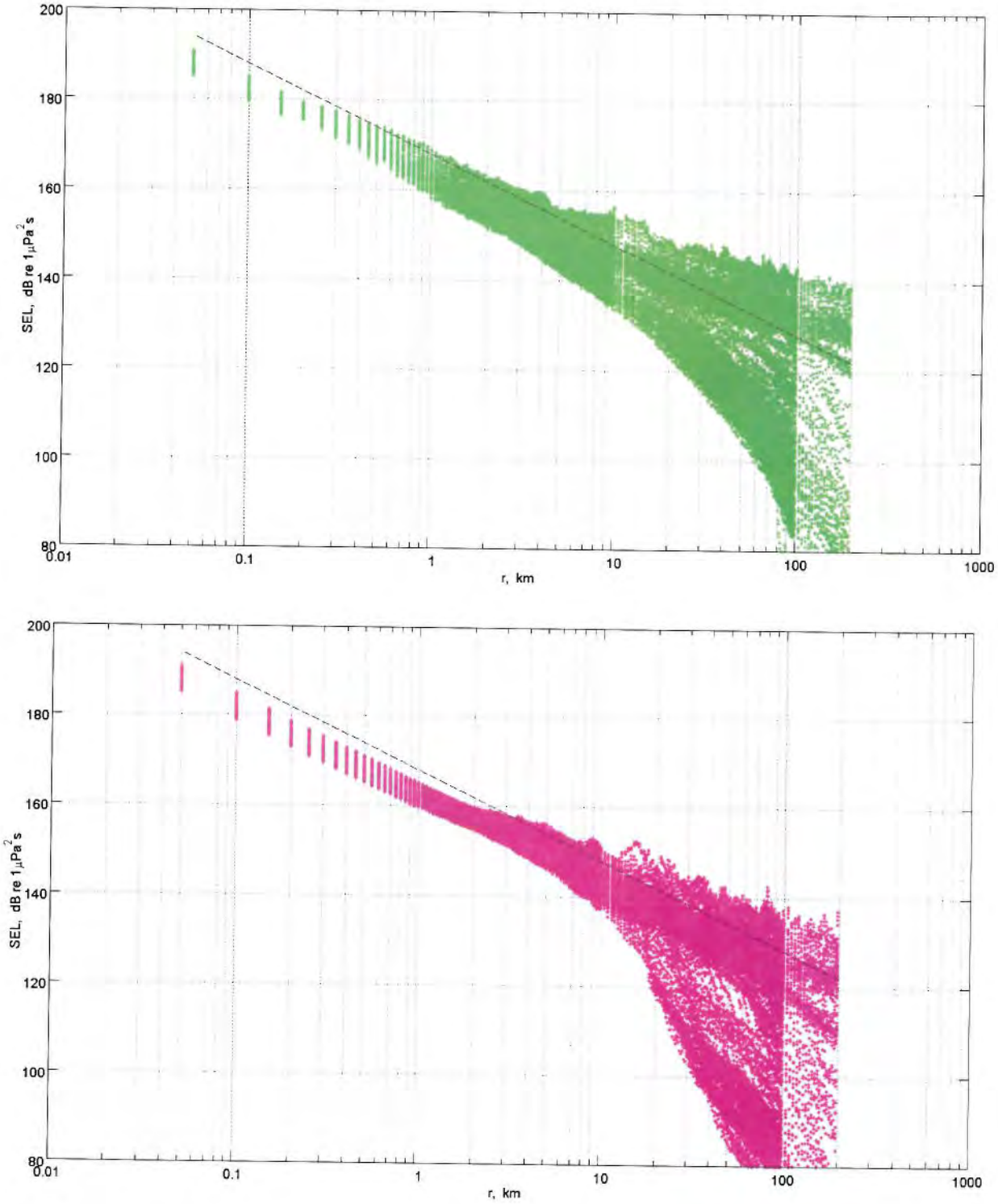

Figure 12: Maximum received sound exposure level at any depth, SEL_{max}, versus range for the points in the centre of the survey area with the PGS 3090 in^3 array: (P2) on 200 m contour (top panel) and (P3) on the 2000 m contour (bottom panel). Black dashed line is 228 – spherical spreading loss.

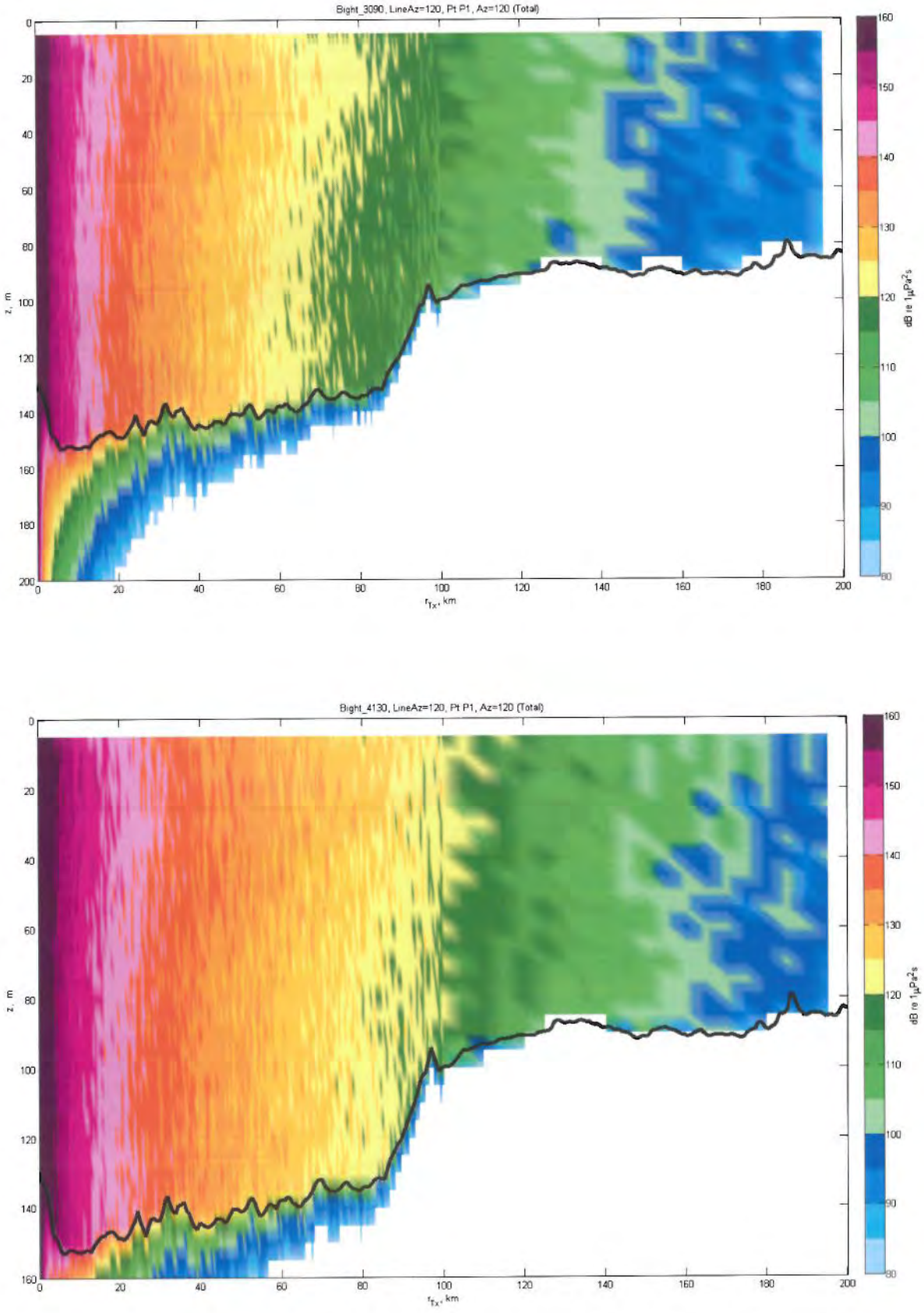

Figure 13: SEL in the vertical plane for (P1) along an azimuth of 120° (i.e. straight ahead) for the PGS 4130 in^3 array (top panel) and PGS 3090 in^3 array (bottom panel). Depth profile shown as a black line.

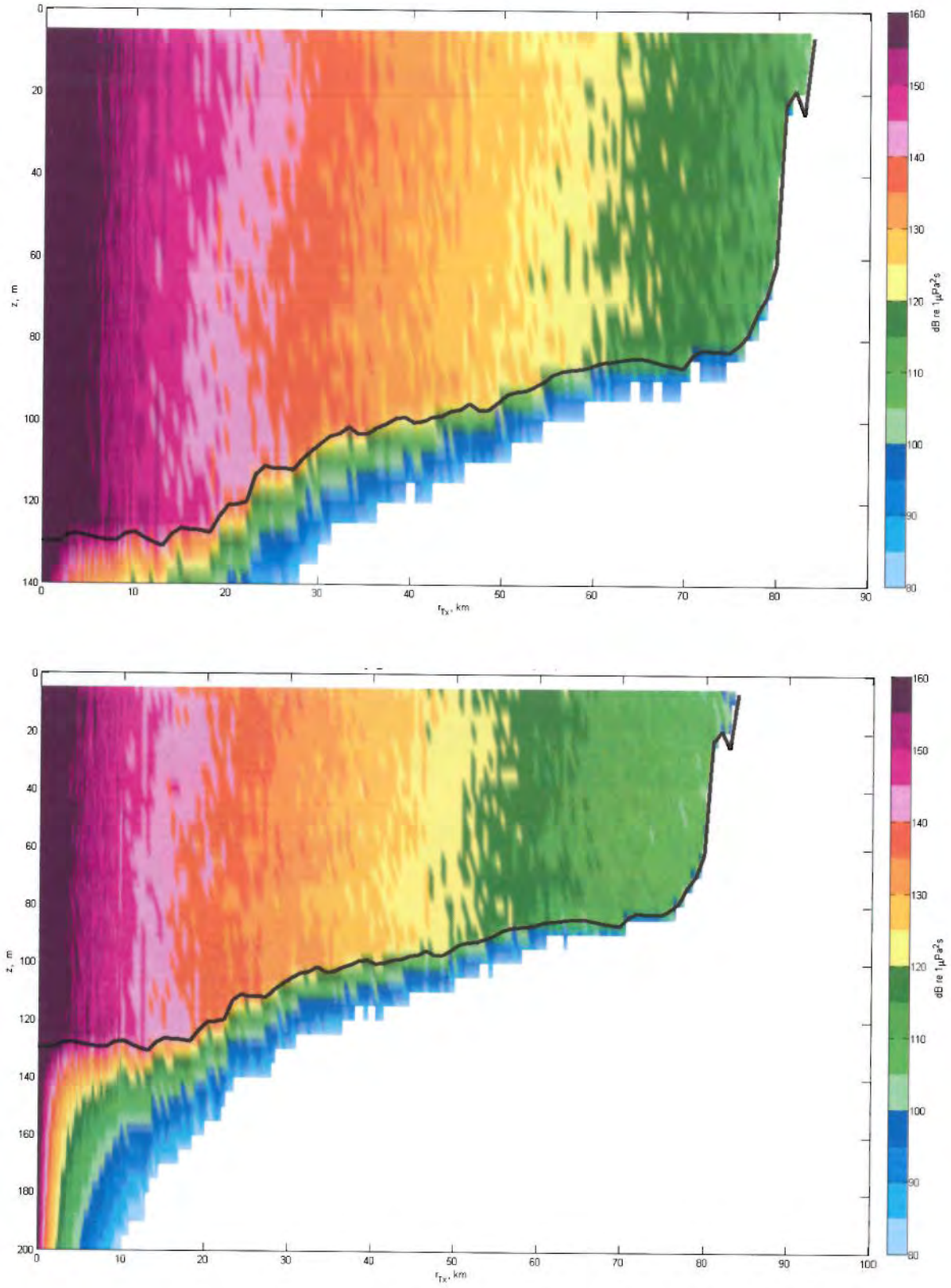

Figure 14: SEL in the vertical plane for (P1) along an azimuth of 30° (i.e. up slope) for the PGS 4130 in^3 array (top panel) and PGS 3090 in^3 array (bottom panel). Depth profile shown as a black line.

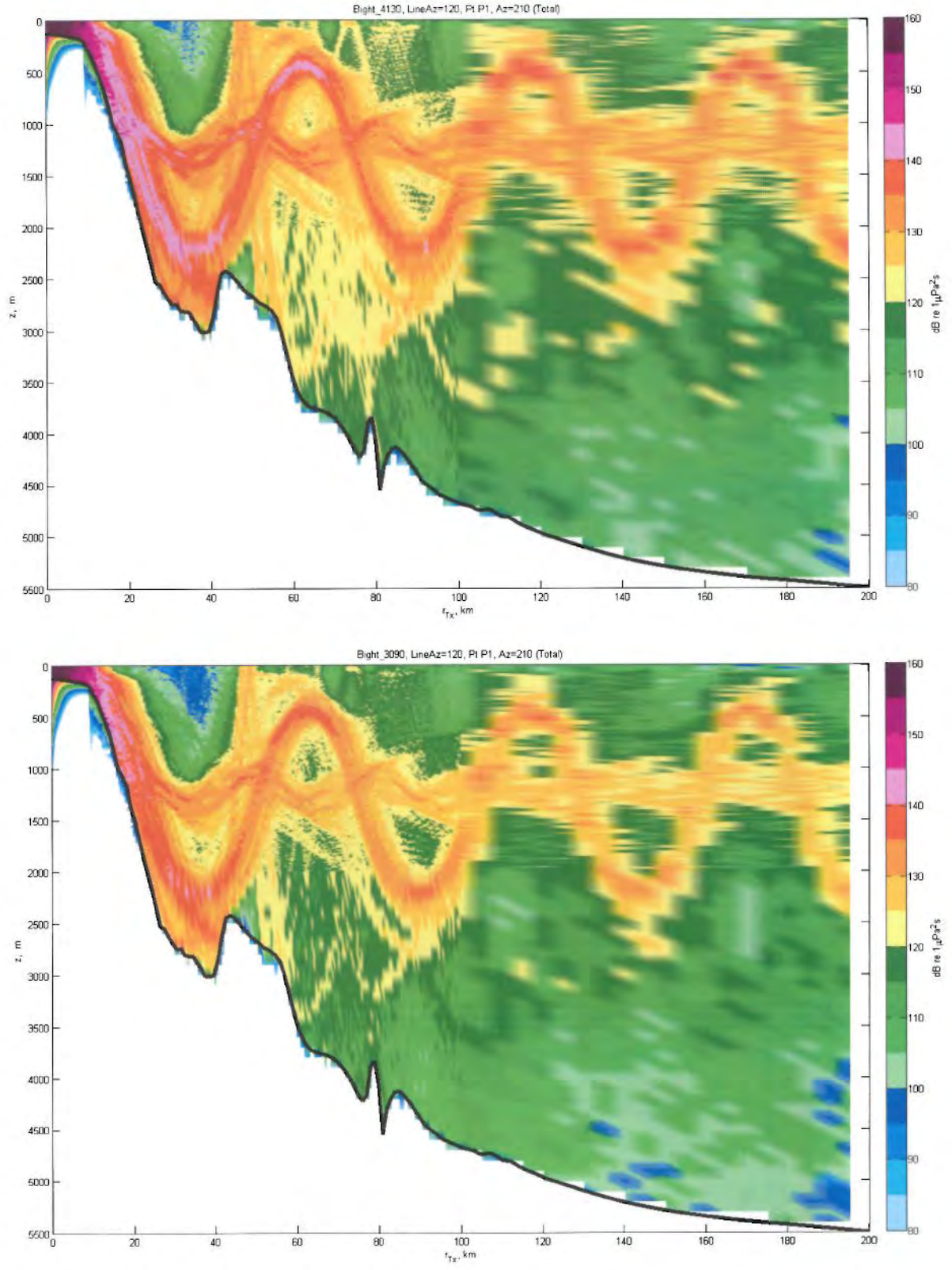

Figure 15: SEL in the vertical plane for (P1) along an azimuth of 210° (i.e. down slope) for the PGS 4130 in^3 array (top panel) and PGS 3090 in^3 array (bottom panel). Depth profile shown as a black line.

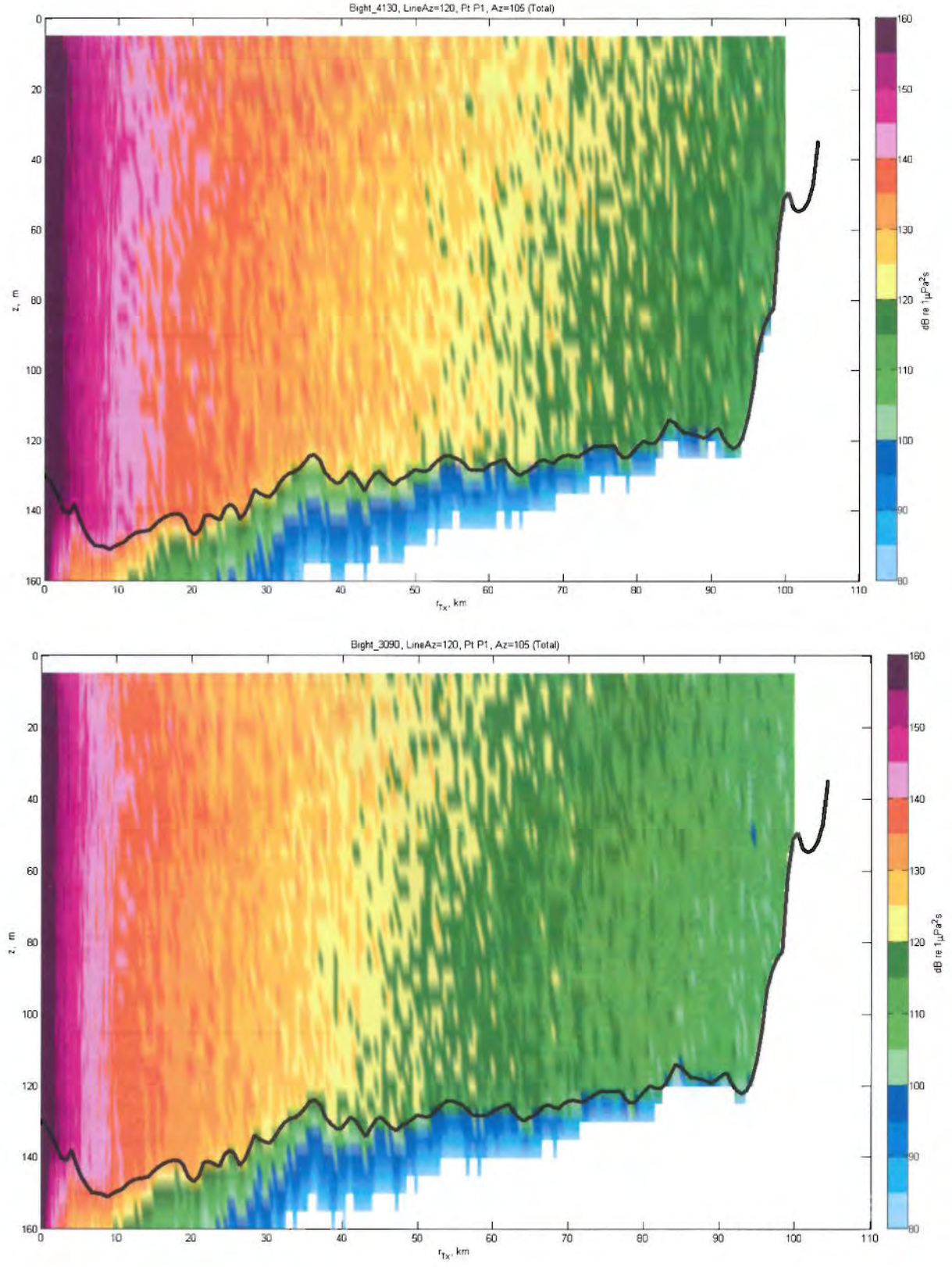

Figure 16: SEL in the vertical plane for (P1) along an azimuth of 105° (i.e. toward KI) for the PGS 4130 in^3 array (top panel) and PGS 3090 in^3 array (bottom panel). Depth profile shown as a black line.

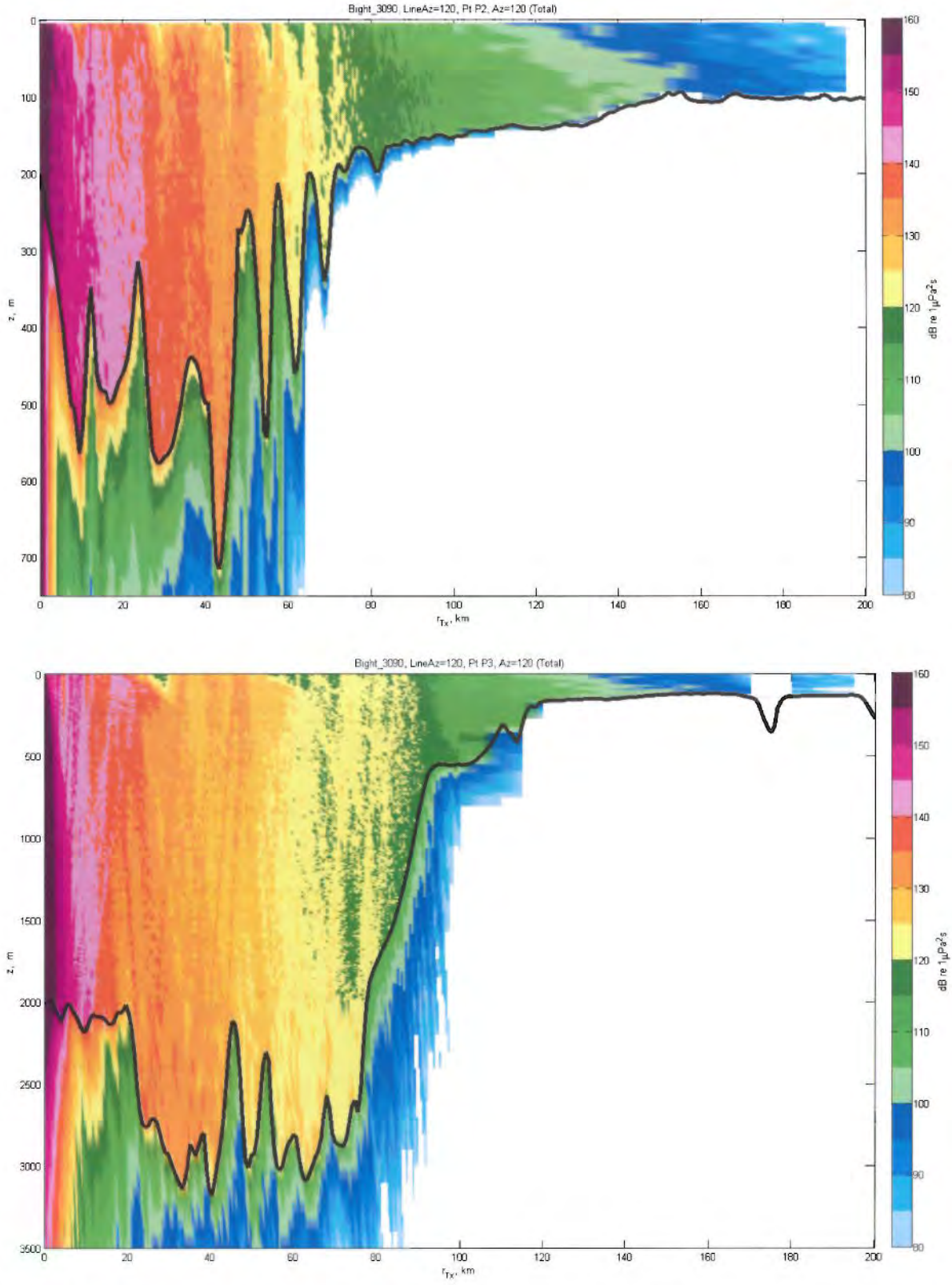

Figure 17: SEL in the vertical plane along an azimuth of 120° (i.e. straight ahead) from the centre of the survey starting at: (P2) the 200 m contour (top panel) and (P3) the 2000 m contour (bottom panel), using the PGS 3090 in^3 array. Depth profile shown as a black line.

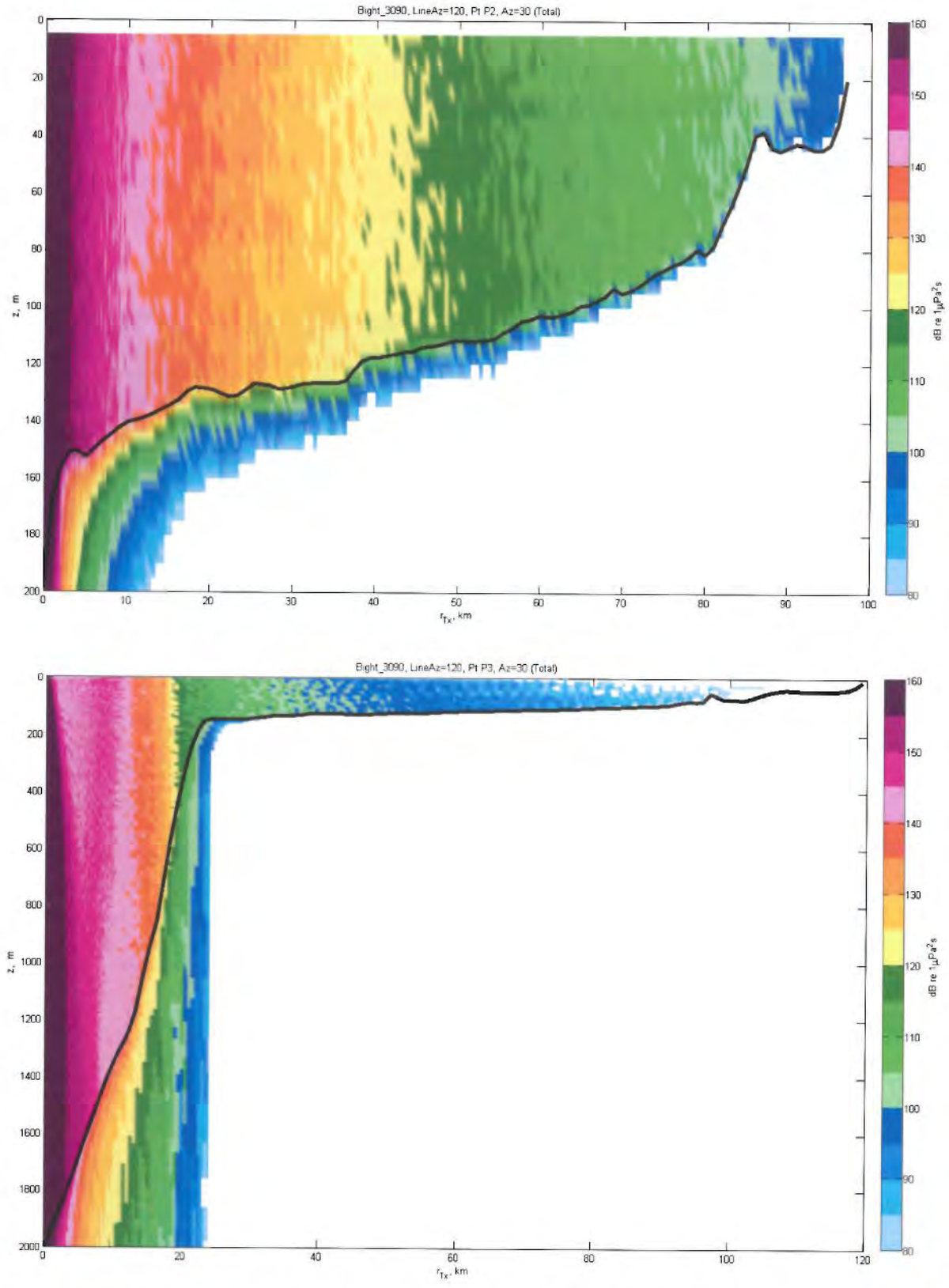

Figure 18: SEL in the vertical plane along an azimuth of 30° (i.e. broadside up slope) from the centre of the survey starting at: (P2) the 200 m contour (top panel) and (P3) the 2000 m contour (bottom panel), using the PGS 3090 in^3 array. Depth profile shown as a black line.

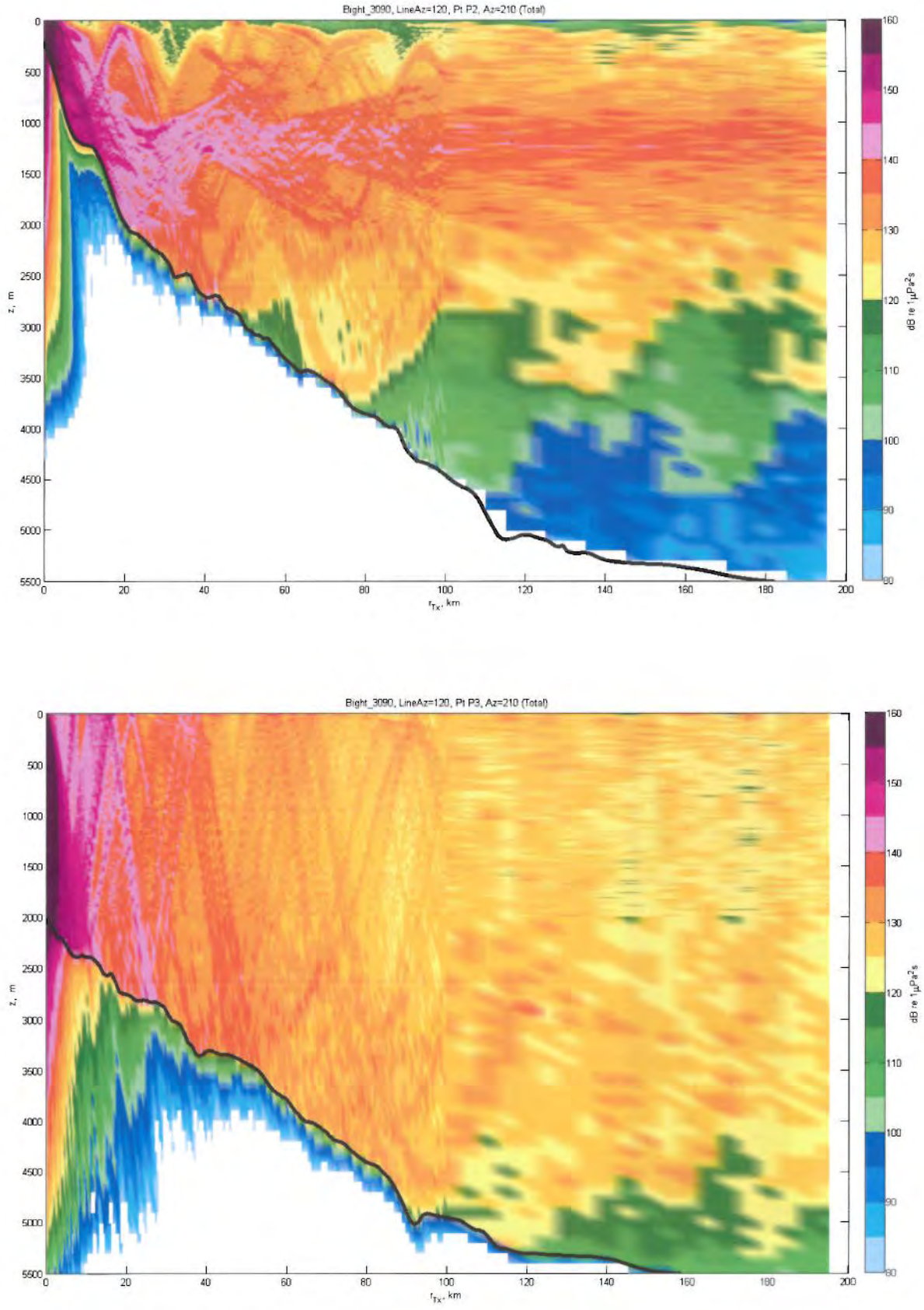

Figure 19: SEL in the vertical plane along an azimuth 21° (i.e. broadside down slope) from the centre of the survey starting at: (P2) the 200 m contour (top panel) and (P3) the 2000 m contour (bottom panel), using the PGS 3090 in^3 array. Depth profile shown as a black line.

4 Conclusions

Received levels of underwater sound have been modelled from 8 to 1000 Hz for three points for the PGS 3090 in^3 array and one point for the PGS 4130 in^3 array, all at a heading of 120° in the proposed survey area in the Eastern Great Australian Bight.

The maximum received SEL drops below 160 dB re 1 $\mu Pa^2.s$ at ranges varying between 800 m and 7 km depending on the location of the source and the direction of propagation. The maximum received SELs at the 50 m contour just off the coast of Kangaroo Island (KI) are predicted to be less than 120 dB re 1 μPa^2s, with the smaller array producing received levels approximately 5 dB lower than the larger array. Results from modelling indicate that the maximum received SELs just off the coast of the Eyre Peninsula will be less than 120 dB re 1 μPa^2s, with the smaller array again producing received levels approximately 5 dB lower than the larger array.

Received levels are strongly dependent on water depth, seabed slope, and direction relative to the array. In general, the rate of decay inshore is more rapid then along the contour, but this is counteracted to some extent by the effect of the array directivity, which results in higher source levels in the inshore direction.

Received levels in the offshore direction show a slower decay rate, particularly when sound energy is coupled into the deep sound channel. The array source level is also at its maximum in the offshore direction. The combination of these two factors results in relatively high received levels for a given range.

Received levels calculated using the modelled source locations should be representative of those that would be produced by the same seismic sources at other locations with similar water depths and seabed slopes.

References

Hamilton, E. L., (1980). *Geoacoustic modeling of the sea floor*, JASA, **68** (5), pp 1313-1340.

Jensen, F. B., Kuperman, W. A., Porter, M. B., Schmidt, H. (2000). *Computational Ocean Acoustics*, Springer-Verlag, N.Y., 2000, ISBN 1-56396-209-8.

Johnson, D. T. (1994), *Understanding airgun bubble behaviour*, Geophysics, **59** (11), 1994, pp 1729-1734.

NOAA (2005), *World Ocean Atlas*, National Oceanic and Atmospheric Administration, National Environmental Satellite, Data, and Information Service 61-62, U.S. Government Printing Office, Washington, D.C., 182 pp, CD-ROM